International Journal of Pharmaceutics 573 (2020) 118798

Contents lists available at ScienceDirect

International Journal of Pharmaceutics

journal homepage: www.elsevier.com/locate/ijpharm

Effect of hydrophobic tails of plier-like cationic lipids on nucleic acid delivery and intracellular trafficking

Supusson Pengnam[a], Samawadee Plainwong[b], Prasopchai Patrojanasophon[a], Theerasak Rojanarata[a], Tanasait Ngawhirunpat[a], Widchaya Radchatawedchakoon[c], Nattisa Niyomtham[d], Boon-ek Yingyongnarongkul[d], Praneet Opanasopit[a,*]

[a] Pharmaceutical Development of Green Innovations Group (PDGIG), Faculty of Pharmacy, Silpakorn University, Nakhon Pathom 73000, Thailand
[b] Faculty of Pharmaceutical Sciences, Burapha University, 20131, Thailand
[c] Creative Chemistry and Innovation Research Unit, Department of Chemistry and Center of Excellence for Innovation in Chemistry (PERCH-CIC), Faculty of Science, Mahasarakham University, MahaSarakham 44150, Thailand
[d] Department of Chemistry and Center of Excellence for Innovation in Chemistry, Faculty of Science, Ramkhamhaeng University, Bangkok 10240, Thailand

ARTICLE INFO

Keywords:
Plier-like cationic lipid
Asymmetry hydrophobic tail
Cationic niosomes
Gemini cationic lipids
DNA and siRNA delivery
Internalization pathway

ABSTRACT

In the optimization of transfection efficacy, one of the crucial barriers to effective gene delivery is in fact the intracellular trafficking of nucleic acids, besides the first and the last steps of gene transfer, i.e., delivery to the cell and transcription. Modifications of cationic lipid structure have been reported to have a significant effect on gene delivery. Therefore, the plier-like cationic lipids (PCLs) have been synthesized and the effect of the different types of hydrophobic tails (chain length and unsaturated hydrocarbon) on physicochemical properties, cellular uptake, trafficking process, transfection, and silencing efficiency has been investigated. In this study, the plier-like cationic niosomes (PCNs) containing PCL (A, B, and C) were evaluated their performance to deliver pDNA and siRNA to HeLa cells. Among the PCNs, PCN-B with saturated asymmetric hydrocarbon tails (C18 and C12) provided the highest efficiency for pDNA and siRNA delivery. Furthermore, the results revealed that the structure of the cationic lipids affected the internalization pathway and the intracellular trafficking. PCL-B and PCL-C with asymmetric tails preferred clathrin- and caveolae-mediated endocytosis as the predominant internalization pathways and were also involved in the polymerization process for transfection. However, PCL-A with symmetry hydrocarbon tails (C12) was predominantly taken up via macropinocytosis. All PCNs were able to escape from endosomal–lysosomal systems through facilitation of acidification. Results obtained from the cytotoxicity test revealed that the PCNs were safe in vitro. Therefore, PCNs provide a great prospect as an alternative effective gene delivery system.

1. Introduction

Gene therapy has been investigated continuously for almost five decades. Scientists believe that genetic modification might become a novel opportunity in the medical field to fulfill the gaps of unachievable treatments for several genetic disorders (Razi Soofiyani et al., 2013). The challenge of gene therapy is the development of efficient gene transfer vectors, which can be categorized into two groups, viral and nonviral. Although viral vectors have been the desired approach in approximately two-thirds of the trials, the primary limitations of viral vectors toward development are safety concerns and the relatively small capacity. In recent years, there has been an expanding use of nonviral vectors in trials conducted till date due to their strengths, including ease of chemical characterization, simplicity and reproducibility of use, larger packaging capacity, and reduced biosafety concerns. Due to these reasons, it has been expected that improved nonviral vectors could be candidates for potential gene delivery systems (Ginn et al., 2018).

Lipofection has been intensively investigated and applied in 4.5% of all gene delivery trials. Lipofection is known as lipid-based transfection, which is constructed as lipid bilayer vesicles behaving like a cell membrane and can carry both hydrophobic and hydrophilic molecules, including nucleic acids, into cells (Carter and Shieh, 2015; Ginn et al., 2018). Niosomes were invented to imitate the bilayer of liposomes. Niosomes are primarily composed of nonionic surfactants (i.e., Span and Tween) that are used instead of phospholipids in liposomes, with

* Corresponding author.
E-mail address: opanasopit_p@su.ac.th (P. Opanasopit).

https://doi.org/10.1016/j.ijpharm.2019.118798
Received 5 July 2019; Received in revised form 2 October 2019; Accepted 13 October 2019
Available online 20 November 2019
0378-5173/

assistance of cholesterol (Chol) for bilayer rigidity (Karim et al., 2010; Paecharoenchai et al., 2013; Amoabediny et al., 2018). To allow the complex formation by electrostatic interaction with the negative charge of nucleic acids, cationic lipids are also incorporated into vesicles as charge inducers. Distinctive points of niosomes compared with liposomes are cost-effective and exhibit better chemical stability against both oxidation and temperature for introduction into pharmaceutical manufacturing (Pardakhty and Moazeni, 2013; Opanasopit et al., 2017; Pei Ling et al., 2018). Paecharoenchai et al. successfully formulated Non-ionic surfactant based vesicles (niosomes) consisted of Span 20, Chol, and spermine derivative cationic lipids that not only exhibited similar physical properties as those of liposomes but also efficiently transferred pDNA with low cytotoxicity and hemolytic activity into HeLa cells (Paecharoenchai et al., 2014; Opanasopit et al., 2017).

Modifications of the cationic lipid structure involve three components, cationic head, linker, and hydrophobic tail, which have been considerably investigated, since relatively little structural changes might affect their physicochemical properties and biological activity (Semple et al., 2010). The hydrophobic tail is commonly a double alkyl chain or a cholesterol derivative. Extensive evidence regarding the double alkyl chain alteration indicates that generally 12–18 carbon units are essential for fusogenic characters and intermembrane mixing between delivery systems and cell membrane, including endosomal escape ability (Martin et al., 2005). Although shorter alkyl lengths, asymmetric alkyl chains, and unsaturated alkyl chains facilitate transfection, their application is still under conflict due to different cell types, composition of vesicles, and cationic lipid structures (Heyes et al., 2002). Gemini cationic lipids, which are a subclass of cationic lipids combined with Chol and 1, 2-di-(9Z-octadecenoyl)-sn-glycero-3-phosphoethanolamine (DOPE), were efficiently applied for plasmid DNA (pDNA) delivery in HeLa cells involving mitochondrial genetic diseases (Cardoso et al., 2015). Gemini cationic surfactants or gemini cationic lipids are composed of identical lipid monomers connected by a rigid spacer. The basic structural design of gemini cationic lipids exhibits membrane destabilization properties, including superior surface interfaces to bind and compact nucleic acids from double cationic heads, which massively contribute to gene transfer (Kirby et al., 2003; Junquera and Aicart, 2016).

As shown in Fig. 1, novel gemini cationic lipids with a plier-like head have been developed possessing ethylenediamine head groups with an alkyl amine spacer connected to 12- or 18-carbon units of alkyl chains by amide bonds. In our previous study, we had successfully formulated A novel cationic lipid as cationic niosomes that exhibited high transfection and silencing efficiency (Pengnam et al., 2019). Herein, our research group emphatically investigates the further effect of symmetric, asymmetric and asymmetric with a double bond modification in alkyl chains on gemini cationic lipids to enhance the efficacy of gene delivery systems. The studies on gemini cationic niosomes for nucleic acid delivery are still limited. Therefore, in this study, the gemini cationic niosomes were formulated from PCL with different hydrophobic tails for pDNA and siRNA delivery. The genes encoding green fluorescent protein were used as a gene target model in this study, which include pDNA encoding green fluorescent protein (pEGFP-C2) and anti-GFP siRNA (siGFP). The physicochemical properties, including the size, surface charge, and nucleic acid condensation, were also investigated. Furthermore, the cellular activities, including the transfection efficiency of DNA, the silencing efficiency of siRNA, cellular uptake, and the internalization pathway, were evaluated using HeLa cells.

2. Material and method

2.1. Materials

Plier-like cationic lipids (PCLs) containing PCL (A, B, and C) were obtained from assistance of Ramkhamhaeng University and Mahasarakham University, Thailand (Fig. 1). Cholesterol (Chol) was acquired from Carlo Erba Reagent (MI, Italy). Span20, 3-(4,5-dimethylthiazol-2-yl)-2, 5-diphenyl tetrazolium bromide (MTT) and inhibitors in the experiment of internalization pathway were purchased from Sigma-Aldrich (St. Louis, Missuori, USA). siRNA AF488 (siAF488) was obtained from Qiagen (Santa Clarita, California, USA). Lipofectamine® 2000 (Lipo2k), LysoTracker™ Red DND-99, Quant-iT™ PicoGreen dsDNA Reagent, ProLong™ Diamond Antifade Mountant, Wheat Germ Agglutinin, tetramethylrhodamine conjugate (WGA-TC), Hoechst 33342, and trihydrochloride were purchased from Invitrogen (Carlsbad, California, USA). Modified Eagle medium (MEM) and fetal bovine serum (FBS) were purchased from GIBCO (San Diego, California, USA).

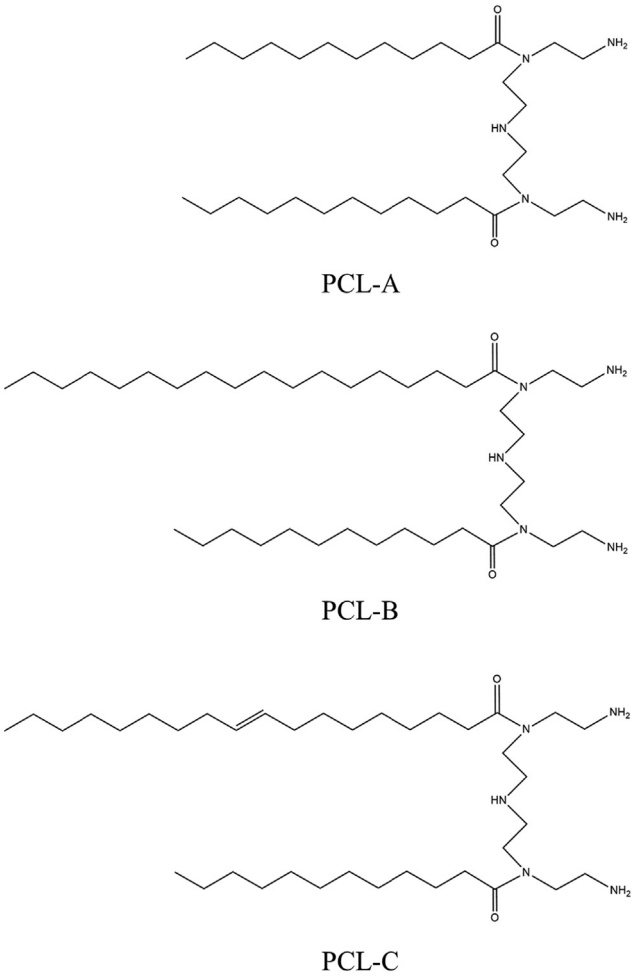

Fig. 1. The structure of plier-like cationic lipids; PCL-A, PCL-B, and PCL-C.

2.2. Preparation of niosomes and nioplexes

The cationic niosomes used in this study were prepared from plier-like cationic lipids (PCL-A, PCL-B, and PCL-C), Span20, and Chol. PLC was dissolved in a methanol:chloroform mixture (1:2 %v/v). Span20 and Chol were dissolved in a methanol:chloroform mixture (1:1 %v/v). Then, each stock solution was mixed together to obtain the molar ratio of PCL:Span20:Chol at 2:2.5:2.5 mM. The solvent was removed by evaporation under N_2 gas to generate a thin film and dried in a desiccator overnight. Tris-buffered saline (pH 7.4) was warmed at 60 °C to swell the film. To reduce the particle size, niosomes were sonicated by a probe sonicator for 30 min (2 cycles) in an ice bath and centrifuged at 15,000 rounds per minute for 15 min to obtain a clear solution. To prepare the nioplexes, the niosomes were incubated with nucleic acids

(pDNA or siRNA) at niosomes-to-nucleic acid weight ratios of 0.1:1, 0.5:1, 1:1, 2.5:1, 5:1, 10:1, 15:1, and 20:1 for 30 min before use in experiments.

2.3. Plasmid DNA preparation

pEGFP-C2 (Clontech, Fremont, California, United States) was used as a reporter gene that was extracted from *Escherichia coli* DH5-α using the DNA purification kit (Qiagen endotoxin-free plasmid purification kit). The concentration of pDNA was measured by NanoDrop™ One/OneC Microvolume UV–Vis Spectrophotometer at 260 nm. PicoGreen-stained pDNA (PG-pDNA) was prepared by incubation of Quant-iT™ PicoGreen dsDNA reagent and pDNA at room temperature for 5 min before the test.

2.4. siRNA synthesis

The sequences of siGFP and noncoding siRNA (siNC) were designed as follows: sense strand: 5′-GCUGACCCUGAAGUUCAUCUU-3′, antisense strand: 5′-GAUGAAC UUCAGGGUCAGCUU-3′, and sense strand: 5′-GCACCGCUUACGUGAUACUUU-3′, antisense strand: 5′-AGUAUCAC GUAAGCGGUGCUU-3′, respectively (Plianwong et al., 2013). Invitrogen's Silencer siRNA Construction Kit was used to synthesis the siRNA for targeting the enhanced green fluorescent protein (EGFP) at the position of the open reading frame (124–144).

2.5. Characterization of niosomes and nioplexes

The niosomes and nioplexes were diluted 100 times in distilled water, and then their particle size and zeta potential were evaluated by Zetasizer Nano obtained from Malvern Instrument. The measurement of each sample (pH 7.4) was performed in triplicate at 25 °C.

2.6. Agarose gel electrophoresis

Gel retardation assay was performed to observe the condensation ability of nioplexes. The samples were loaded onto an agarose gel (0.8% for DNA complexes or 1% for siRNA complexes), which was submerged in a running buffer (1X Tris-acetate-EDTA buffer for DNA complexes or 1X Tris-borate-EDTA buffer for siRNA complexes). DNA ladder (1 kb) from GeneDireX was also loaded. The electricity source was controlled using a power supply at 100 V for 45 min. Ethidium bromide was used for gel staining before the gel was imaged under UV light using a gel doc system.

2.7. Maintaining cell culture

HeLa cells and HeLa–EGFP stable cells were used in this study. The cells were grown in complete MEM (MEM containing 1% of non-essential amino acid solution, 100 mg/mL of streptomycin, 100 U/mL of penicillin, 1% of L-glutamine and 10% of FBS) under the condition of 37 °C with 5% CO_2 to maintain the cells. For HeLa cells stably expressing EGFP cells (HeLa–EGFP), pEGFP-C2 was delivered by Lipo2k and then the cells were treated with 0.1 mg/mL G418 every 3 weeks for maintaining EGFP expression.

2.8. Gene transfection

The transfection efficiency of nioplexes was calculated according to Eq. (1) using HeLa cells in a 48-well plate. A day before treating the cells, the cells contained in complete MEM were added to each well at a density of 1×10^4 cells and incubated under normal conditions. The medium was replaced with nioplexes contained in serum-free medium (0.5 μg/well of DNA containing) and incubated for 24 h. Complete MEM was added to each well after washing the cells with phosphate-buffered saline (PBS). After 48 h of incubation, GFP was observed using an inverted fluorescence microscope, followed by analysis using the ImageJ software (Model: GFP-B, wavelengths: emission filter 535/50 and excitation filter 480/40). Positive control and negative control were also operated using the Lipo2k/pEGFP-C2 complex at a weight ratio of 2 and pEGFP-C2, respectively. The calculation of % transfection efficiency was computed using Eq. (1).

The cationic niosomes which exhibited the high transfection efficiency was selected for the evaluation by Flow Cytometer (BD FACSCanto™, BD Bioscience, USA). HeLa cells were seeded into 24-well plates at a density of 3×10^4 cells/cm^2, and were supplied with the nioplexes using the same procedure as for the in vitro transfection experiment. After 48-h incubation, the cells were collected by trypsinization followed by fixation with 4% formaldehyde prior to the flow cytometry analysis.

$$\%\ \text{Transfection efficiency} = \frac{[\text{Transfected cells}_{\text{nioplexes}} - \text{Transfected cells}_{\text{negative control}}] \times 100}{[\text{Transfected cells}_{\text{Lipo2k}} - \text{Transfected cells}_{\text{negative control}}]} \quad (1)$$

2.9. Gene silencing

The gene silencing efficiency of GFP was examined using HeLa–EGFP cells that were seeded into a 96-well black clear-bottom plate at a density of 9000 cells/well and incubated under normal conditions for 24 h. The medium was changed as serum-free medium, and the fluorescence intensity was analyzed at day 0 by Fluoroskan™ Microplate Fluorometer. The cells were treated with the complexes of niosomes/siGFP or Lipo2k/siGFP (at the weight ratio of 2.5), which presented 15 pmol/well of siRNA for 24 h. siNC was also transfected by the transfection agent for calculating the gene silencing efficiency as described previously (Opanasopit et al., 2010). The percentages of silencing efficiency were calculated using Eq. (2).

$$\%\ \text{silencing efficiency} = \frac{(I_{siNC} - I_{siGFP}) \times 100}{I_{siNC}} \quad (2)$$

I_{siGFP} is the fluorescence intensity of siGFP transfection
I_{siNC} is the fluorescence intensity of siNC transfection

2.10. Cytotoxicity of niosomes and nioplexes

The cytotoxicity test of niosomes and nioplexes was conducted using a HeLa cell line by MTT assay. Cells were seeded at a density of 10,000 cells/well in a 96-well plate. After 24 h of incubation, the samples in the serum-free medium were added to the plate and incubated continuously under normal conditions for 24 h. Untreated cell control was also performed simultaneously. Then, the cells were rinsed with PBS and replaced with completed MEM before incubating with MTT, with the final concentration being 0.5 mg/mL/well, for 3 h. Subsequently, the medium was replaced with 100 μL of dimethyl sulfoxide (DMSO) for dissolving the formazan crystal. The percentage of cell viability and the half maximal inhibitory concentration (IC50) were computed from absorbance at a wavelength of 550 nm by comparison with the control that was defined as 100% cell viability. The absorbance was measured at 550 nm by VICTOR Nivo® Multimode Microplate Reader, PerkinElmer.

2.11. Cellular uptake analysis

HeLa cells were seeded into a 24-well plate at a density of 3×10^4 cells/well in complete MEM for a day before transfection and incubated under normal conditions. The serum-free medium containing the niosome complexes or Lipo2k/siAF488 complex were transferred to the cells and incubated for 24 h. The cells were cleansed twice with PBS

and detached using trypsin. Then, 4% formaldehyde in PBS was added and rapidly mixed with the cell suspension and then preserved at 4 °C until analysis. The cells were analized using BD FACSCanto™ Flow Cytometer, BD Bioscience (Becton and Dickinson and Company) to obtain % cellular uptake and % mean fluorescence intensity (MFI) which was calculated using Eq. (3).

$$\%\mathrm{MFI} = \frac{[\mathrm{MFI}_{\mathrm{nioplexes}} - \mathrm{MFI}_{\mathrm{control}}] \times 100}{[\mathrm{MFI}_{\mathrm{Lipo2k}} - \mathrm{MFI}_{\mathrm{control}}]} \quad (3)$$

2.12. Internalization pathways of nioplexes

Nioplexes of DNA and siRNA internalization pathways were investigated using HeLa cells. Specific endocytosis inhibitors were applied to the cells for 30 min before transfection that was further performed through the same processes as the previous experiments (gene transfection and gene silencing). The mechanism of nioplexes was delineated using 50 nM of wortmannin (PI3-kinase inhibition of macropinocytosis), 1 mM of methyl-β-cyclodextrin (chol depletion of cell membrane), 5 μM of chlorpromazine (specific inhibition of clathrin-mediated endocytosis by dissociation of clathrin lattice), 10 μM of genistein (tyrosine-phosphorylation inhibition of caveolae-mediated endocytosis), 10 μM of filipin (specific inhibition of caveolae-mediated endocytosis by Chol binding), 10 nM nacodazol (inhibition of microtubule depolymerization) and 20 mM of ammonium chloride (pH increase of late endosomes and lysosomes). The time-course cellular association of nucleic acid transfection and the effect of specific internalization inhibitors of nucleic acids on the cellular association were performed, and the findings are presented in supplementary information.

2.13. Confocal laser scanning microscopy (CLSM)

Sterilized coverslips were placed at the bottom of a 24-well plate. HeLa cells were seeded at a density of 30,000 cells/well for 24 h. The optimal weight ratios of PCN/siAF488 and PCN/PG-pDNA, in which siAF488 and PG-pDNA were fixed at 30 pmol/well (0.42 μg/well), and 1 μg/well, respectively were incubated to the cells for 24 h. The cells were cleansed three times with PBS. Then, 5 μg/mL of WGA-TC and 5 μg/ mL of Hoechst 33,342 were mixed together. Next, 200 μL/well of the mixture was applied to the cells for staining the plasma membrane and the nucleus for 15 min. For colocalization analysis, the optimal weight ratios of PCN/PG-pDNA and 60 nM of LysoTracker™ Red DND-99 (for lysosomal staining) were applied to the cells for different durations (30 min and 2 h). The cells were cleansed three times with PBS before being stained by 5 μg/mL of Hoechst 33,342 for 15 min. After staining, the cells were cleansed three times with PBS before fixing with 4% formaldehyde in PBS for 15 min. The coverslips were taken out of the well and air-dried before mounting on a glass slide by ProLong™ Diamond Antifade Mountant. Cell imaging was conducted using 60x oil immersion objective in FV10i confocal laser scanning microscope, Olympus.

2.14. pH titrations of cationic niosomes

pH titration of cationic noisomes was performed to evaluate the buffer capacity of the niosomes using the modified procedure from literature (Gabrielson and Pack, 2006). The niosomes were diluted to obtain 1 mg/mL of total lipids. 25 kDa polyethyleneimine (PEI) was dissolved in water (1 mg/mL) as a positive control. The pH of the niosomes and PEI (1 mL) were adjusted to 11.5 using 1 N sodium hydroxide. The solutions were then titrated dropwise with 1 N hydrochloric acid (titrant). The pH of solution was measured using a pH meter (LAQUAtwin pH-22, Irvine, CA, USA). Afterwards, the titration curve between pH and volume of the titrant added was plotted.

Table 1
Mean particle size, polydispersity index (PDI) and zeta potential of PCNs. The data are presented as the mean ± SD of triplicates.

PCNs	Size (nm)	PDI	Zeta potential (mV)
PCN-A	155.1 ± 1.2	0.204 ± 0.019	56.7 ± 2.5
PCN-B	141.3 ± 7.5	0.233 ± 0.032	54.8 ± 0.2
PCN-C	144.4 ± 3.2	0.226 ± 0.012	54.9 ± 2.2

2.15. Statistical analysis

Statistical analyses were conducted using Microsoft Excel 2016 MSO for Windows. The data of all experiments are reported as mean ± standard deviation, which was analyzed using F-test and independent T-test, respectively, at a significance level of $p < 0.05$.

3. Results and discussion

3.1. The morphology of niosomes and nioplexes

The plier-like cationic niosomes (PCNs) were formulated from Span20 and Chol, at a molar ratio of 2.5:2.5 mM, and 2 mM of the novel cationic lipids with different chain lengths or unsaturated hydrophobic tails (PCL-A, PCL-B, and PCL-C) as shown in Fig. 1. The particle sizes and the zeta potentials of the PCNs are shown in Table 1. The particle sizes of all formulations were ~150 nm, and the zeta potentials were ~ (+) 55 mV. The particle sizes and the zeta potentials of nioplexes (PCN/pEGFP) are presented in Fig. 2. The amount of cationic niosomes varied in terms of the weight ratio of niosomes-to-nucleic acids. DNA and siRNA were defined with constant weights of 0.5 and 0.14 μg, respectively. The niosomes could establish complexes with nucleic acids by electrostatic attraction as depicted in Fig. 2a. The zeta potential was increased when the weight ratios of cationic niosomes-to-DNA or siRNA increased. The feature of all nioplexes had three different zones, negative, neutral, and positive (Desigaux et al., 2007; Schroeder et al., 2010). Firstly, the particle sizes of DNA nioplexes slightly decreased to that of stable colloidal complexes, ranging from 464 to 193 nm at the weight ratios of 0.5–5 and were in the nanosize. This was due to their higher density of protonated amines in the cationic niosomes. However, the zeta potentials were of negative charge. Secondly, the particle size of DNA nioplexes dramatically increased to that of unstable colloidal complexes to more than 3000 nm, and the zeta potential was almost neutral or transformed into a slight positive charge when the weight ratio was increased to 10. Lastly, at higher weight ratios, the particle size became smaller complexes and exhibited more positive charges than those at lower ratios. This was attributed to the intermolecular interaction between DNA strands by self-aggregates with an excess amount of cationic niosomes. A similar result was observed in previous studies (Wang et al., 2007; Weecharangsan et al., 2008; Paecharoenchai et al., 2012) This finding implies that these cationic niosomes were able to condense DNA into a compact size (Chen et al., 2007). Furthermore, the feature of siRNA nioplexes was similar to DNA nioplexes, but siRNA nioplexes required more weight ratios for condensation, probably due to the lower binding strength of cationic niosomes to siRNA. A similar result was observed in previous studies (Chang Kang and Bae, 2011; Bolcato-Bellemin et al., 2007). Bolcato-Bellemin et al. (2007) discussed that the complex formation of many siRNA molecules with a polycationic polymer such as polyethylenimine (PEI) molecule or a liposome favored intracomplex encounter of siRNAs and shielded their repulsive forces. The resulting gene-like concatemers had a much larger overall electrostatic interaction with the delivery vector, hence were less prone to exchange with other polyanions. As shown in Fig. 2b, the weight ratios of siRNA nioplexes ranged between 1 and 10 and were in the first zone. The siRNA nioplexes required a weight ratio of > 15 to become positively charged.

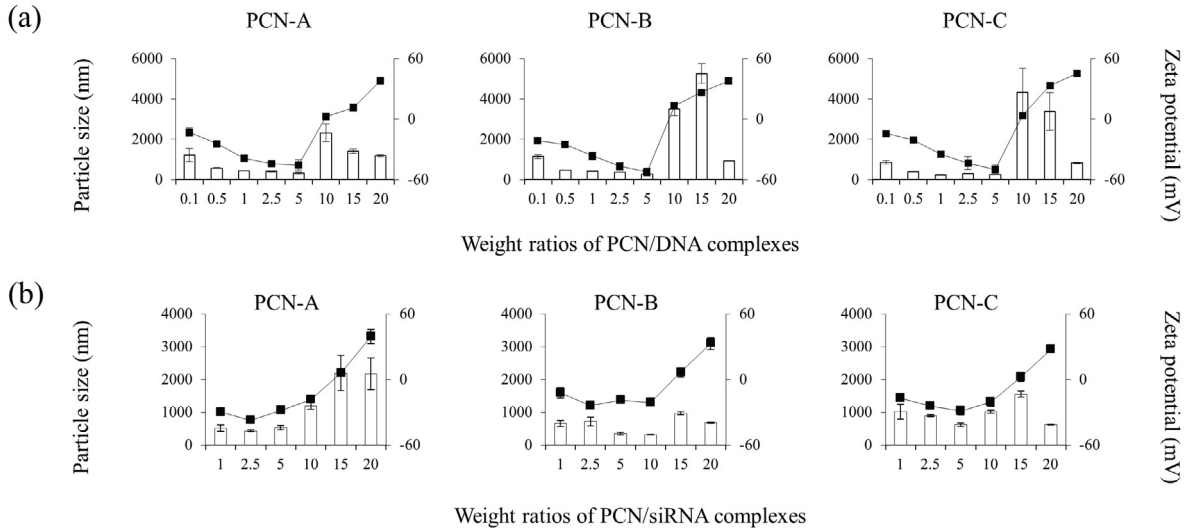

Fig. 2. The particle size and the zeta potential of (a) PCN/DNA complexes at the weight ratios of 0.1–20 and (b) PCN/siRNA complexes at the weight ratios of 1–20.

3.2. Gel retardation assay

The ability of niosomes to condense nucleic acids was observed by agarose gel electrophoresis. Various weight ratios between nioplexes and nucleic acids were evaluated. An incomplete complexation was determined based on the observation of nucleic acid bands remaining on the agarose gel under UV light. The niosomes could completely condense DNA and siRNA at the weight ratios of 10 and 15, respectively, which were retarded in the wells (Fig. 3a, b). Although the physical structure of DNA and siRNA is a phosphodiester backbone, the length of nucleotides is not equal. The size of pEGFP-C2 is approximately 4.7 kb, whereas that of siRNA or small RNA is about 20 bp. The short strand characteristic makes them more rigid, with a higher rotational and translational degree of freedom but less electrostatic repulsion than pEGFP-C2, which is an abundant and flexible macromolecule. In addition, the cationic niosomes have to overcome the free energy of siRNA (Bouxsein et al., 2007; Li and Szoka, 2007; Scholz and Wagner, 2012; Zhang et al., 2013). Therefore, siRNA is required in higher cationic niosome concentration to condense it into stable complexes.

3.3. Transfection efficiency and silencing efficiency

The transfection efficiency of niosomes was evaluated using pEGFP-C2 encoding the GFP as a reporter gene to transfect in HeLa cells. To

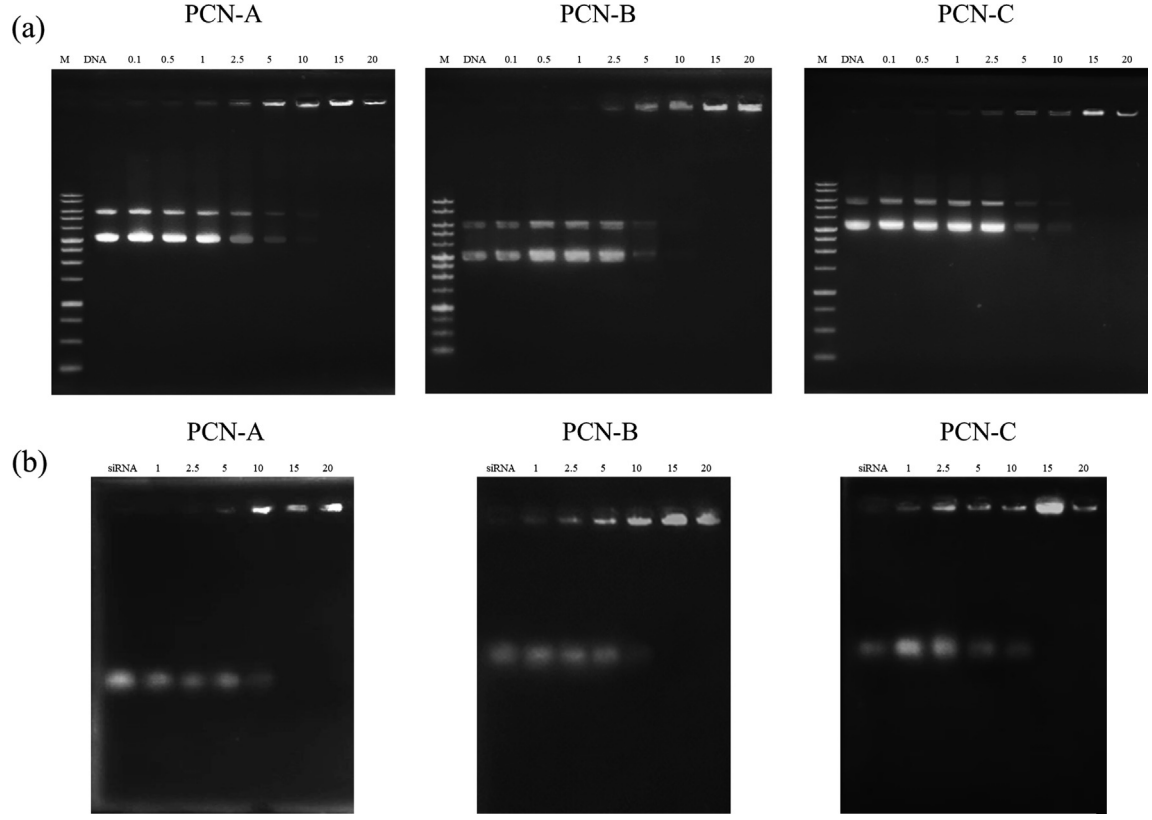

Fig. 3. Gel retardation assays of (a) PCN/DNA complexes at the weight ratios of 0.1–20 and (b) PCN/siRNA complexes at the weight ratios of 1–20.

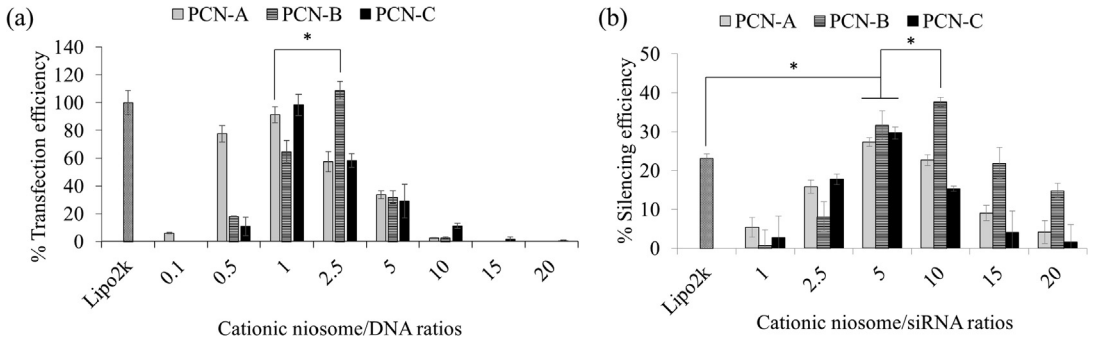

Fig. 4. Transfection efficiency of (a) PCN/DNA complexes at the weight ratios of 0.1–20 and silencing efficiency of (b) PCN/siRNA complexes at the weight ratios of 1–20. Lipo2k was used as a positive control. *Statistically significant at $p < 0.05$.

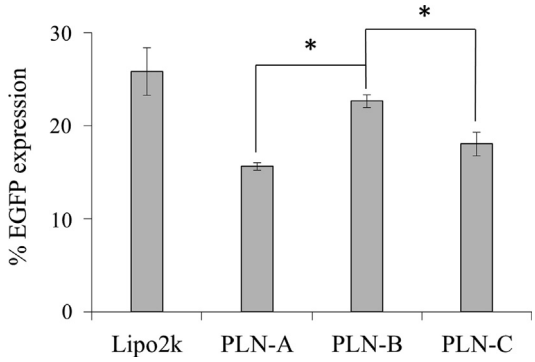

Fig. 5. EGFP expressions of (a) PCN-A/DNA complexes, PCN-B/DNA complexes and PCN-C/DNA complexes at the weight ratios of 5, 5 and 10, respectively. Lipo2k was used as a positive control. *Statistically significant at $p < 0.05$.

calculate the relative percentage of transfection efficiency, Lipo2k was also used as positive control (100% transfection efficiency). The weight ratios of niosomes were varied to obtain the effective activity. The results shown in Fig. 4a indicate that the optimal weight ratios of PCN-A, PCN-B, and PCN-C were 1 (91.24% ± 5.67%), 2.5 (108.72% ± 6.48%), and 1 (98.37% ± 7.79%), respectively, of which PCN-B exhibited the most effective transfection. The optimal weight ratio of each PCN for EGFP expression was also evaluated by flow cytometry, and the results are depicted in Fig. 5. The percentages of EGFP expression sequence of the PNCs was consistent with an observation by inverted fluorescence microscope, which the expression of PNC-B, PCN-C and PCN-A were 22.63 ± 0.68%, 18.03 ± 1.24% and 15.63 ± 2.55%, respectively. Moreover, the silencing efficiency of niosomes was examined by delivery of siGFP into HeLa–EGFP stable cells for GFP silencing as a study model as shown in Fig. 4b. The effective weight ratios of niosomes were different from the transfection efficiency study, i.e., the weight ratios of PCN-A, PCN-B, and PCN-C were 5 (25.38% ± 1.75%), 10 (37.73% ± 1.50%), and 5 (29.68% ± 2.14%), respectively, among which PCN-B showed a significantly superior silencing efficiency. The results also showed that asymmetric alkyl chains of cationic lipids possess more efficiency than the symmetry alkyl chains. One of keys to successful transfection is endosomal membrane perturbations for releasing nucleic acids into the environment. The asymmetric hydrocarbon chains could facilitate fusogenicity (Martin et al., 2005). In addition, a lower nucleic acid disassembly rate is obtained with symmetry (Saker and Takeoka, 2018). We hypothesized that hydrocarbon chain with double bond might enhance the transfection efficiency by increasing the fluidity of the membrane bilayer through intermembrane mixing (Martin et al., 2005; Koynova et al., 2009; Saker and Takeoka, 2018). However, our study found that the presence of hydrocarbon chain with double bond did not improve the efficiency of the asymmetric novel synthesized gemini cationic lipids. This might be because some nioplexes of PCN-C were broken before the intermembrane mixing circumstances due to the double bond in hydrocarbon chain that increased the fluidity. Furthermore, the lipid arrangement of the arch lipid (double bond area) was highly difficult for packing with other compositions, which could be the cause of the unstable bilayer. The saturated asymmetric hydrocarbon chain of gemini cationic lipids remained overhanging on the hydrophobic tail to connect between both sides of the bilayer through Van der Waals forces which caused the aligned area (Heyes et al., 2002; Meka et al., 2016). The saturated asymmetric could increase the membrane integrity of the gemini niosomes and protect the early breakdown of the vesicles (Nantz et al., 2010). Gemini lipids have a spacer between monomer lipids, which also provides fluidity to the bilayer system. Therefore, a balance between fluidity and rigidity of the bilayer system is required for cationic lipid designs.

3.4. Evaluation of cytotoxicity

The cytotoxicity of niosomes and nioplexes was evaluated by the MTT assay. The IC_{50} values of all niosomes were investigated and found to be in the following order: PCN-B (36.16 ± 0.98 μg/mL), PCN-A (29.13 ± 0.19 μg/mL), and PCN-C (28.93 ± 0.55 μg/mL). The DNA nioplexes of PCN-A and PCN-C at weight ratios < 5 were less toxic, wherein the cell viability was > 80%. However, the cytotoxicity of PCN-B was observed at a weight ratio > 10, which exhibited < 80% of cell viability (Fig. 6a). Regarding the cell viability of siRNA nioplexes shown in Fig. 6b, the cells were able to tolerate the toxicity of PCN-A and PCN-C at the weight ratio < 10 and that of PCN-B at the weight ratio < 20, wherein the cell viability was > 80%. These results revealed that the shorter chain lipids are associated with toxicity (Koynova et al., 2009). The saturated asymmetric hydrocarbon chains provided less cytotoxicity compared with the unsaturated chains. The cytotoxicity of the unsaturated hydrocarbon chains might be one of the reasons for their diminished efficiency. The increase in cationic lipids could be the cause of cytotoxicity. However, the most effective weight ratios of all formulations (PCN-A/DNA (1:1), PCN-B/DNA (2.5:1), PCN-C/DNA (1:1), PCN-A/siRNA (5:1), PCN-B/siRNA (10:1) and PCN-C/siRNA (5:1)), exhibited a negligible cytotoxicity which could be safe and potential transfection agents for both DNA and siRNA.

3.5. Cellular uptake analysis by CLSM and flow cytometry

Cellular uptake analysis was performed, and the CLSM images are shown in Fig. 7. The PNCs could deliver pDNA to the target site which were partially inside the nucleus (Fig. 7a). Primarily, both Lipo2k and cationic niosomes could deliver siRNA into the cytoplasm where it is the typical area for siRNA to regulate the mRNA level by interrupting the translation process. Furthermore, the PCN-B delivery system was considerably taken up by HeLa cells, which can be observed from the amount of green fluorescence complex of siAF488 (Fig. 7b). The results from CLSM were consistent with flow cytometry interpretation. The

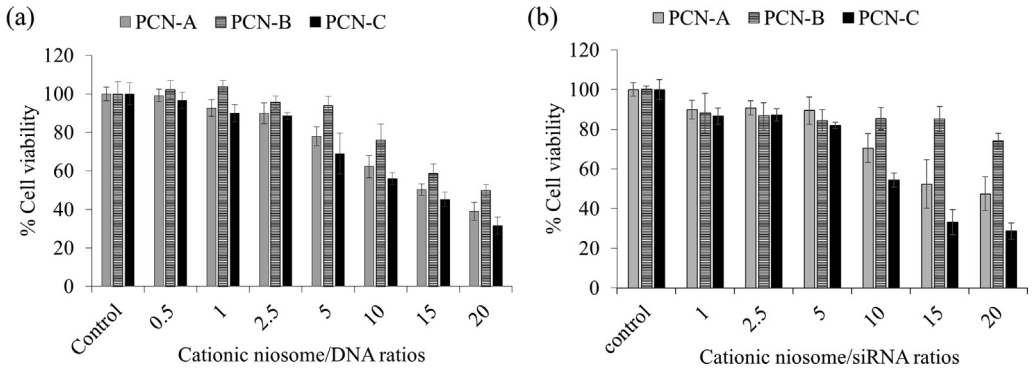

Fig. 6. Viability of HeLa cells treated with (a) PCN/DNA complexes at the weight ratios of 0.1–20 and (b) PCN/siRNA complexes at the weight ratios of 1–20.

cellular uptake efficiency of niosomes was also investigated by flow cytometry, and the results are shown in Fig. 8a, depicting that the cellular internalization of Lipo2k, PCN-A, PCN-B, and PCN-C was almost 100% with no significant difference. MFI was also calculated using the MFI of Lipo2k, which indicated 100% intensity, to compare the carrier capacity with the optimal weight ratios of each niosome (Fig. 8b). The MFI of Lipo2k was two and three times higher than that of PCN-A and PCN-C, respectively, at the weight ratio of 5. Although Lipo2k could carry more siRNA to the cells than PCN, the silencing efficiency was lower. It has been reported that SPANosomes showed a superior rate of siRNA release into cytosol than Lipo2k (Zhou et al., 2012). Jain S et al. revealed that the binding of spermine was established by enclosing spermine to the major groves of nucleotides (Jain et al., 1989; Balazs and Godbey, 2011). Thus, the spermine of Lipo2k in the cationic lipid head might delay the nucleic acid release, which affected their activities. PCN-B at the weight ratio of 10 exhibited the highest MFI, which could deliver siAF488 into the cell by more than three times compared with Lipo2k and approximately seven times compared with PCN-A and PCN-C at the weight ratio of 5. This result suggested that the cellular uptake ability of PCN-B was not limited by the cytotoxicity at a higher weight ratio, and therefore, PCN-B could carry more siRNA into the cells and subsequently exhibited an effective activity.

3.6. Internalization pathways of nioplexes

Nanocarriers generally are taken up by endocytosis as the major route across the plasma membrane (Sahay et al., 2010; Vercauteren et al., 2012). After entry into cells as intracellular vesicles or endosomes, they would finally incorporate with lysosomes and degraded if the carrier is not able to release nucleic acids to their target site. To clarify the predominant internalization pathway and how hydrophobic tails of PCN might trigger the different pathways, the cells were pretreated with specific endocytosis inhibitors and then the DNA nioplexes or the siRNA nioplexes at the effective weight ratio of each lipid in the previous experiment were applied. The possible internalization pathways were ruled out by comparing their activity between cells pretreated with specific endocytosis inhibitors and cells untreated with inhibitors.

The results shown in Fig. 9 indicated that the activity of PCN systems decreased by pretreatment with ammonium chloride (inhibited endosome acidification). Therefore, it could be concluded that endosomal–lysosomal acidification was required for PCN escape. For DNA delivery (Fig. 9a), it was found that wortmannin, methyl-β-cyclodextrin, and chlorpromazine significantly ($p < 0.05$) affected the transfection efficiency of all nioplexes. PCN-A delivered pEGFP-C2 through micropinocytosis as a major internalization pathway, followed by

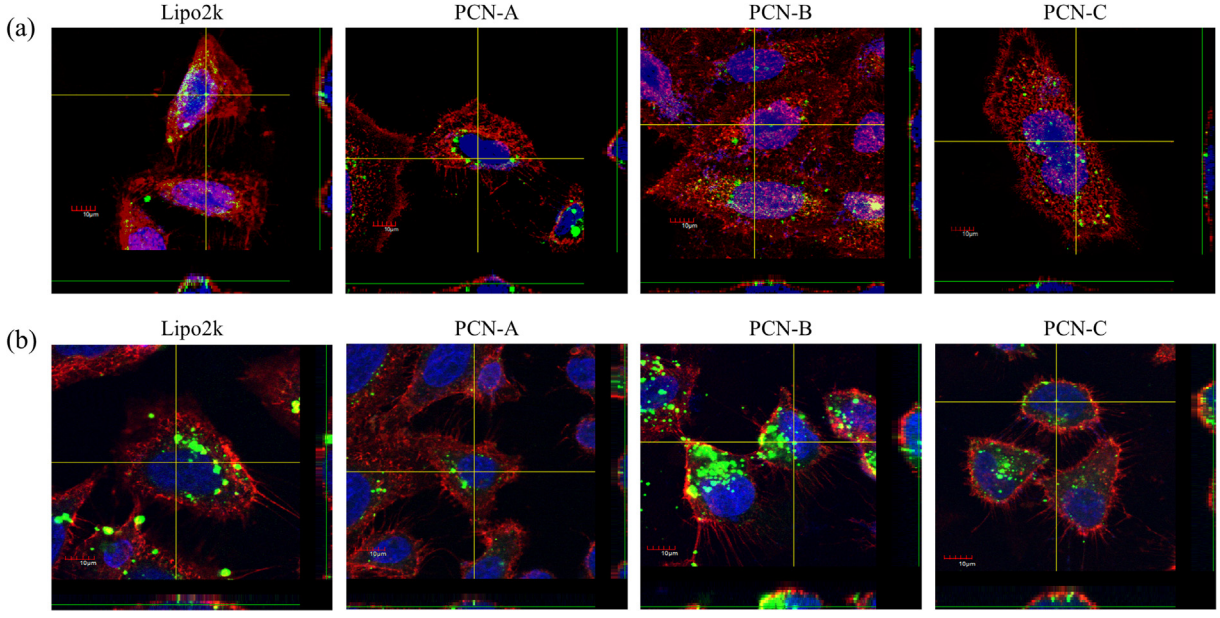

Fig. 7. CLSM images showing perpendicular three planes through HeLa cells of (a) PCN/DNA complexes (green) (PCN-A/DNA complexes, PCN-B/DNA complexes and PCN-C/DNA complexes at the weight ratios of 5, 5 and 10, respectively) and (b) PCN/siRNA complexes (green) (PCN-A/siAF488, PCN-B/siAF488, and PCN-C/siAF488 complexes at the weight ratios of 5, 10, and 5, respectively). The cells were stained with WGA-TC (red) for plasma membrane and with Hoechst 33342 (blue) for nucleus. Lipo2k was used as a positive control.

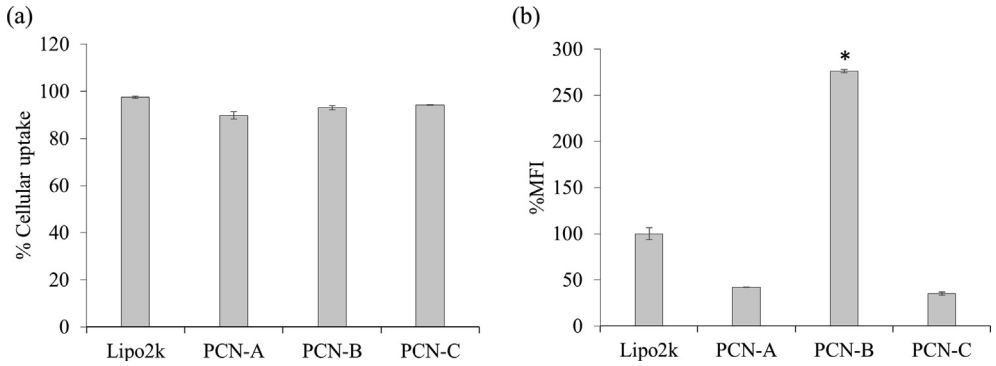

Fig. 8. (a) Cellular uptakes and (b) MFI of PCN-A/siRNA, PCN-B/siRNA, and PCN-C/siRNA complexes at the weight ratios of 5, 10, and 5, respectively. Lipo2k was used as a positive control. *Statistically significant at $p < 0.05$.

clathrin- and caveolae-mediated endocytosis as minor pathways. Although macropinosome has been mentioned that it is easy to escape from the vesicle, the delivery system could be partially degraded by the lysosomal incorporation (LeCher et al., 2017). However, DNA delivery of PCN-B and PCN-C was almost similar; they used clathrin-mediated endocytosis as a predominant internalization pathway, followed by caveolae-mediated endocytosis and micropinocytosis, respectively. However, PCN-C did not significantly involve caveolae-mediated endocytosis. For siRNA delivery, the internalization pathway of all nioplexes was associated with micropinocytosis and clathrin- and caveolae-mediated endocytosis (Fig. 9b). The internalization pathway of siRNA delivery was depicted about the same with DNA delivery. The major internalization pathways of asymmetric niosomes were clathrin- and caveolae-mediated endocytosis, while micropinocytosis was a minor pathway.

Remarkably, pretreatment with methyl-β-cyclodextrin, which depleted chol from cell membrane, showed the most inhibitory effect on both DNA and siRNA delivery. Chol is important for cell membrane ruffle formation, which is involved in the endocytosis of extracellular macromolecules, including micropinocytosis and caveolae- and clathrin-mediated endocytosis (Rodal et al., 1999; Rodal et al., 1999; Fielding and Fielding, 2000, 2003; Ormerod et al., 2012; Mahammad and Parmryd, 2015). Furthermore, nioplexes with asymmetric hydrocarbon chains were different from niosomes with symmetry chains because their activities were inhibited by nocodazole. The intracellular pathway and the intracellular trafficking of the asymmetric hydrocarbon chains were dependent on the polymerization of microtubules, which is essential for vesicle transport and machinery recycling. Thus, the travel of nioplexes with asymmetric chains might be obstructed before reaching the target site, and machinery recycling was inhibited when pretreated with nocodazole. On the other hand, they might be interrupted during passive transportation of mitosis-cell division (dos Santos et al., 2011; Mayle et al., 2012). However, investigation of the exact internalization pathway has been laborious till date.

3.7. Colocalization and buffer capacity

The colocalization images between the lysosome stained with LysoTracker Red (red fluorescent dye) and the PCN-B/DNA complexes at the weight ratio of 2.5 (green fluorescent) were depicted in Fig. 10a to observe the endosomal escape ability of PCN-B. The CLSM images showed that the DNA complexes of PCN-B were found in lysosome (red arrows), suggesting that the complexes were taken up to endosome and fused with lysosome after 30 min of transfection. Interestingly, the green fluorescent could dissociate from the red fluorescent which was indicated by the white arrows, indicating that the DNA complexes of PCN-B could escape from endosome after 2 h of transfection (Lin et al., 2019). Regarding the proton sponge hypothesis, the buffer capacity is important for endosomal escape ability. PEI is a well-known polymer having proton sponge effect (Gabrielson and Pack, 2006; Creusat et al., 2010). The pKa value of PEI is between neutral and endosomal pH which can buffer acidification of endosomal vesicles. Therefore, balancing of ion was controlled by counter ion influx (chloride) when a nitrogen atom was further protonated in the endosome. This event caused endosomal swelling and bursting followed by release of nioplexes to the environment. We hypothesized those tertiary amides on the PCNs, which exhibit lower pKa values than the corresponding primary and secondary amines, can act as proton acceptors and provide

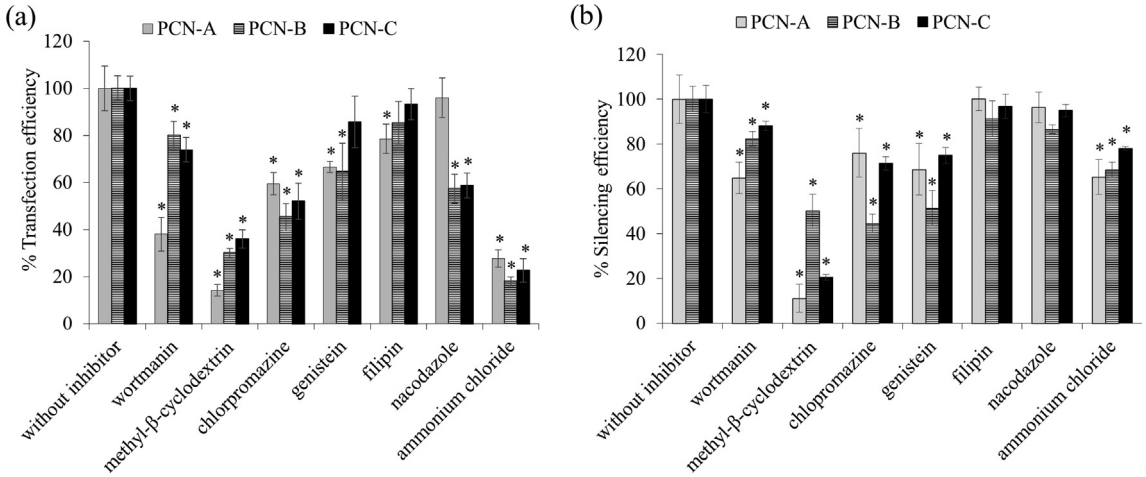

Fig. 9. Effect of specific internalization pathway inhibitors on (a) transfection efficiency of PCN/DNA complexes and (b) silencing efficiency of PCN/siRNA complexes. *Statistically significant at $p < 0.05$ between the treatments of DNA of siRNA complexes without inhibitor and with specific inhibitors.

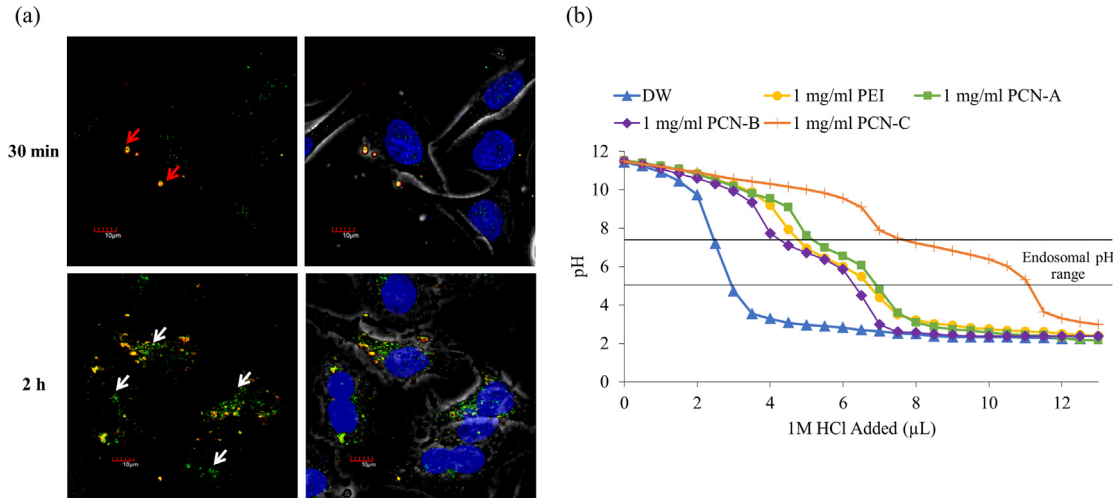

Fig. 10. (a) The colocalization between lysosome stained with LysoTracker Red (red fluorescent dye) and DNA complexes of PCN-B at the weight ratio of 2.5 (green fluorescent), is indicated by red arrows (at 30 min of transfection). The escape of DNA complexes from the lysosome (at 2 h of transfection) is indicated by a white arrow. The cells were stained with Hoechst 33342 (blue) for nucleus. (b) Acidic titration curves of PCNs. PEI and DW were used as a positive control and negative control, respectively.

proton sponge effect to the systems (Liang and Lam, 2012). Therefore, the buffer capacity of PCNs was expressed by the slope of acidic titration curve over the pH range of endosome, which was depicted in Fig. 10b. The PCNs demonstrated buffer capacity indicated by a gradual slope in the endosomal pH range. The flattest slope between pH 5 to 7.4 indicated the greatest endosomal buffer capacity. The result revealed that PCN-C exhibited the highest buffer capacity with a slope of 3.4 μL (of 1 N HCl/pH unit). On the other hand, PCN-A provided the lowest buffer capacity with a slope of about 1.77 μL over the pH range. The PCN-B showed a similar buffer capacity to PEI which the slope over the pH range was 2.08 μL and 1.92 μL, respectively. However, the transfection efficiency was not increased as the buffer capacity increased. Gabrielson and Pack found that the increase in the degree of acetylation of PEI resulted in a declined buffer capacity. However, no change in the transfection efficiency was observed as the degree of acetylation of PEI increased. This is because acetylation appears to enhance the dissociation of polyplexes and release DNA to the target site (Gabrielson and Pack, 2006). Although a buffer capacity has benefit for proton sponge effect, there are still other factors involve with nucleic acid delivery of the PCNs; for instance, lipid bilayer the integrity and intermembrane mixing of niosomes.

4. Conclusion

This study has revealed that different hydrophobic tails affected the cellular uptake, internalization, and trafficking process, as well as transfection and silencing efficiency, in HeLa cells. PCN-B with saturated asymmetric tails significantly provided the highest transfection efficiency and silencing efficiency. Thus, PCL-B might be a potential cationic lipid candidate to formulate as cationic niosomes for DNA and siRNA delivery. Therefore, these modifications of the cationic lipid structure are the challenges for researchers to further design more potential cationic lipids for efficient nucleic acid delivery.

Declaration of Competing Interest

The authors declare that they have no known competing financial interests or personal relationships that could have appeared to influence the work reported in this paper.

Acknowledgements

The authors would like to acknowledge the financial support from the Thailand Research Fund through the Golden Jubilee Ph.D Program (GrantNo. PHD/0047/2559) and through the Research Team Promotion Grant (RTA6180003), Research and Creative Fund, Faculty of Pharmacy, Silpakorn University and Faculty of Pharmaceutical Sciences, Burapha University. We also would like to gratefully thank the Center of Excellence for Innovation in Chemistry (PERCH-CIC), OHEC, Ministry of Education, Ramkhamhaeng University and Mahasarakham University for the support on cationic lipid.

Appendix A. Supplementary material

Supplementary data to this article can be found online at https://doi.org/10.1016/j.ijpharm.2019.118798.

References

Amoabediny, G., Haghiralsadat, F., Naderinezhad, S., Helder, M.N., Akhoundi Kharanaghi, E., Mohammadnejad Arough, J., Zandieh-Doulabi, B., 2018. Overview of preparation methods of polymeric and lipid-based (niosome, solid lipid, liposome) nanoparticles: a comprehensive review. Int. J. Polym. Mater. Po. 6, 383–400. https://doi.org/10.1080/00914037.2017.1332623.

Balazs, D.A., Godbey, W., 2011. Liposomes for use in gene delivery. J. Drug. Deliv. 326497. https://doi.org/10.1155/2011/326497.

Bolcato-Bellemin, A.L., Bonnet, M.E., Creusat, G., Erbacher, P., Behr, J.P., 2007. Sticky overhangs enhance siRNA-mediated gene silencing. Proc. Natl. Acad. Sci. USA 104, 16050–16055. https://doi.org/10.1073/pnas.0707831104.

Bouxsein, N.F., McAllister, C.S., Ewert, K.K., Samuel, C.E., Safinya, C.R., 2007. Structure and gene silencing activities of monovalent and pentavalent cationic lipid vectors complexed with siRNA. Biochemistry 16, 4785–4792. https://doi.org/10.1021/bi062138l.

Cardoso, A.M., Morais, C.M., Cruz, A.R., Cardoso, A.L., Silva, S.G., do Vale, M.L., Marques, E.F., Pedroso de Lima, M.C., Jurado, A.S., 2015. Gemini surfactants mediate efficient mitochondrial gene delivery and expression. Mol. Pharm. 3, 716–730. https://doi.org/10.1021/mp5005349.

Carter, M., Shieh, J., 2015. Gene Delivery Strategies. In: Carter, M., Shieh, J. (Eds.). E-Publishing Inc., San Diego, pp. 239–252 (Chapter 11).

Chang Kang, H., Bae, Y.H., 2011. Co-delivery of small interfering RNA and plasmid DNA using a polymeric vector. Biomaterials 32, 4914–4924. https://doi.org/10.1016/j.biomaterials.2011.03.042.

Chen, J.L., Wang, H., Gao, J.Q., Chen, H.L., Liang, W.Q., 2007. Liposomes modified with polycation used for gene delivery: preparation, characterization and transfection in vitro. Int. J. Pharm. 343, 255–261. https://doi.org/10.1016/j.ijpharm.2007.05.045.

Creusat, G., Rinaldi, A.S., Weiss, E., Elbaghdadi, R., Remy, J.S., Mulherkar, R., Zuber, G., 2010. Proton sponge trick for pH-sensitive disassembly of polyethylenimine-based siRNA delivery systems. Bioconjug Chem. 5, 994–1002. https://doi.org/10.1021/bc100010k.

Desigaux, L., Sainlos, M., Lambert, O., Chevre, R., Letrou-Bonneval, E., Vigneron, J.P., Lehn, P., Lehn, J.M., Pitard, B., 2007. Self-assembled lamellar complexes of siRNA with lipidic aminoglycoside derivatives promote efficient siRNA delivery and interference. Proc. Natl. Acad. Sci. USA 42, 16534–16539. https://doi.org/10.1073/pnas.0707431104.

dos Santos, T., Varela, J., Lynch, I., Salvati, A., Dawson, K.A., 2011. Effects of transport inhibitors on the cellular uptake of carboxylated polystyrene nanoparticles in different cell lines. PLoS One 9, e24438. https://doi.org/10.1371/journal.pone.0024438.

Fielding, C.J., Fielding, P.E., 2000. Cholesterol and caveolae: structural and functional relationships. Biochim. Biophys. Acta. 1–3, 210–222.

Fielding, C.J., Fielding, P.E., 2003. Relationship between cholesterol trafficking and signaling in rafts and caveolae. Biochim. Biophys. Acta. Biomembr. 2, 219–228. https://doi.org/10.1016/S0005-2736(03)00020-8.

Gabrielson, N.P., Pack, D.W., 2006. Acetylation of polyethylenimine enhances gene delivery via weakened polymer/DNA interactions. Biomacromolecules 8, 2427–2435. https://doi.org/10.1021/bm060300u.

Ginn, S.L., Amaya, A.K., Alexander, I.E., Edelstein, M., Abedi, M.R., 2018. Gene therapy clinical trials worldwide to 2017: an update. J. Gene. Med. 5, e3015. https://doi.org/10.1002/jgm.3015.

Heyes, J.A., Niculescu-Duvaz, D., Cooper, R.G., Springer, C.J., 2002. Synthesis of novel cationic lipids: effect of structural modification on the efficiency of gene transfer. J. Med. Chem. 1, 99–114. https://doi.org/10.1021/jm010918g.

Jain, S., Zon, G., Sundaralingam, M., 1989. Base only binding of spermine in the deep groove of the A-DNA octamer d(GTGTACAC). Biochemistry 6, 2360–2364.

Junquera, E., Aicart, E., 2016. Recent progress in gene therapy to deliver nucleic acids with multivalent cationic vectors. Adv. Colloid. Interface. Sci. 161–75. https://doi.org/10.1016/j.cis.2015.07.003.

Karim, K., Mandal, A., Biswas, N., Guha, A., Chatterjee, S., Behera, M., Kuotsu, K., 2010. Niosome: A future of targeted drug delivery systems. J. Adv. Pharm. Technol. Res. 4, 374–380. https://doi.org/10.4103/0110-5558.76435.

Kirby, A.J., Camilleri, P., Engberts, J.B., Feiters, M.C., Nolte, R.J., Soderman, O., Bergsma, M., Bell, P.C., Fielden, M.L., Garcia Rodriguez, C.L., Guedat, P., Kremer, A., McGregor, C., Perrin, C., Ronsin, G., van Eijk, M.C., 2003. Gemini surfactants: new synthetic vectors for gene transfection. Angew. Chem. Int. Ed. Engl. 13, 1448–1457. https://doi.org/10.1002/anie.200201597.

Koynova, R., Tenchov, B., Wang, L., Macdonald, R.C., 2009. Hydrophobic moiety of cationic lipids strongly modulates their transfection activity. Mol. Pharm. 3, 951–958. https://doi.org/10.1021/mp8002573.

LeCher, J.C., Nowak, S.J., McMurry, J.L., 2017. Breaking in and busting out: cell-penetrating peptides and the endosomal escape problem. Biomol. Concepts 3–4, 131–141. https://doi.org/10.1515/bmc-2017-0023.

Li, W., Szoka Jr., F.C., 2007. Lipid-based nanoparticles for nucleic acid delivery. Pharm. Res. 3, 438–449. https://doi.org/10.1007/s11095-006-9180-5.

Liang, W and Lam, J.K.W., 2012. Endosomal escape pathways for non-viral nucleic acid delivery systems. In: Ceresa, B. (Ed.). Molecular regulation of endocytosis. E-Publishing Inc., IntechOpen.

Lin, Y.-L., Chen, C.-H., Liu, Y.-K., Huang, T.-H., Tsai, N.-M., Tzou, S.-C., Liao, K.-W., 2019. Lipo-PEG-PEI complex as an intracellular transporter for protein therapeutics. Int J Nanomed. 1119–30. https://doi.org/10.2147/IJN.S188970.

Mahammad, S., Parmryd, I., 2015. Cholesterol depletion using methyl-beta-cyclodextrin. Methods Mol. Biol. 91–102. https://doi.org/10.1007/978-1-4939-1752-5_8.

Martin, B., Sainlos, M., Aissaoui, A., Oudrhiri, N., Hauchecorne, M., Vigneron, J.P., Lehn, J.M., Lehn, P., 2005. The design of cationic lipids for gene delivery. Curr. Pharm. Des. 3, 375–394.

Mayle, K.M., Le, A.M., Kamei, D.T., 2012. The intracellular trafficking pathway of transferrin. Biochim. Biophys. Acta 3, 264–281. https://doi.org/10.1016/j.bbagen.2011. 09.009.

Meka, R.R., Godeshala, S., Marepally, S., Thorat, K., Reddy Rachamalla, H.K., Dhayani, A., Hiwale, A., Banerjee, R., Chaudhuri, A., Vemula, P.K., 2016. Asymmetric cationic lipid based non-viral vectors for an efficient nucleic acid delivery. RSC. Adv. 81, 77841–77848. https://doi.org/10.1039/C6RA07256A.

Nantz, M.H., Dicus, C.W., Hilliard, B., Yellayi, S., Zou, S., Hecker, J.G., 2010. The benefit of hydrophobic domain asymmetry on the efficacy of transfection as measured by in vivo imaging. Mol. Pharm. 3, 786–794. https://doi.org/10.1021/mp900298f.

Opanasopit, P., Leksantikul, L., Niyomtham, N., Rojanarata, T., Ngawhirunpat, T., Yingyongnarongkul, B.E., 2017. Cationic niosomes an effective gene carrier composed of novel spermine-derivative cationic lipids: effect of central core structures. Pharm. Dev. Technol. 3, 350–359. https://doi.org/10.3109/10837450.2015.1125925.

Opanasopit, P., Techaarpornkul, S., Rojanarata, T., Ngawhirunpat, T., Ruktanonchai, U., 2010. Nucleic acid delivery with chitosan hydroxybenzotriazole. Oligonucleotides 3, 127–136. https://doi.org/10.1089/oli.2009.0227.

Ormerod, K.G., Rogasevskaia, T.P., Coorssen, J.R., Mercier, A.J., 2012. Cholesterol-independent effects of methyl-β-cyclodextrin on chemical synapses. PLoS ONE 5, e36395. https://doi.org/10.1371/journal.pone.0036395.

Paecharoenchai, O., Niyomtham, N., Leksantikul, L., Ngawhirunpat, T., Rojanarata, T., Yingyongnarongkul, B.-E., Opanasopit, P., 2014. Nonionic surfactant vesicles composed of novel spermine-derivative cationic lipids as an effective gene carrier in vitro. AAPS. PharmSciTech. 3, 722–730. https://doi.org/10.1208/s12249-014-0095-x.

Paecharoenchai, O., Niyomtham, N., Ngawhirunpat, T., Rojanarata, T., Yingyongnarongkul, B.-E., Opanasopit, P., 2012. Cationic niosomes composed of spermine-based cationic lipids mediate high gene transfection efficiency. J. Drug. Target. 20, 783–792. https://doi.org/10.3109/1061186X.2012.716846.

Paecharoenchai, O., Teng, L., Yung, B.C., Teng, L., Opanasopit, P., Lee, R.J., 2013. Nonionic surfactant vesicles for delivery of RNAi therapeutics. Nanomedicine. (Lond) 11, 1865–1873. https://doi.org/10.2217/nnm.13.155.

Pardakhty, A., Moazeni, E., 2013. Nano-niosomes in drug, vaccine and gene delivery: a rapid overview. Nanomed. J. 1, 1–12. https://doi.org/10.22038/nmj.2013.697.

Pei Ling, Y., Chooi Ling, L., Soi Moi, C., Anna Pick Kiong, L., Rhun Yian, K., 2018. Niosomes: a review of their structure, properties, methods of preparation, and medical applications. Asian. Biomed. 4, 301–314. https://doi.org/10.1515/abm-2018-0002.

Pengnam, S., Patrojanasophon, P., Rojanarata, T., Ngawhirunpat, T., Yingyongnarongkul, B.-E., Radchatawedchakoon, W., Opanasopit, P., 2019. A novel plier-like gemini cationic niosome for nucleic acid delivery. J. Drug. Deliv. Sci. Technol. 325–33. https://doi.org/10.1016/j.jddst.2019.04.032.

Plianwong, S., Opanasopit, P., Ngawhirunpat, T., Rojanarata, T., 2013. Chitosan combined with poly-L-arginine as efficient, safe, and serum-insensitive vehicle with rnase protection ability for siRNA delivery. B. Biomed. Res. Int. 9. https://doi.org/10.1155/2013/574136.

Razi Soofiyani, S., Baradaran, B., Lotfipour, F., Kazemi, T., Mohammadnejad, L., 2013. Gene therapy, early promises, subsequent problems, and recent breakthroughs. Adv. Pharm. Bull. 2, 249–255. https://doi.org/10.5681/apb.2013.041.

Rodal, S.K., Skretting, G., Garred, Ø., Vilhardt, F., Deurs, B.v., Sandvig, K., 1999. Extraction of cholesterol with methyl-β-cyclodextrin perturbs formation of clathrin-coated endocytic vesicles. Mol. Biol. Cell. 4, 961–974. https://doi.org/10.1091/mbc.10.4.961.

Sahay, G., Alakhova, D.Y., Kabanov, A.V., 2010. Endocytosis of nanomedicines. J. Control. Release. 3, 182–195. https://doi.org/10.1016/j.jconrel.2010.01.036.

Saker, S.R., Takeoka, S., 2018. Amino acid-based liposomal assemblies: intracellular plasmid DNA delivery nanoparticles. J. Nanomed. 1008.

Scholz, C., Wagner, E., 2012. Therapeutic plasmid DNA versus siRNA delivery: common and different tasks for synthetic carriers. J. Control. Release 2, 554–565. https://doi.org/10.1016/j.jconrel.2011.11.014.

Schroeder, A., Levins, C.G., Cortez, C., Langer, R., Anderson, D.G., 2010. Lipid-based nanotherapeutics for siRNA delivery. J. Intern. Med. 1, 9–21. https://doi.org/10.1111/j. 1365-2796, 2009.02189.x.

Semple, S.C., Akinc, A., Chen, J., Sandhu, A.P., Mui, B.L., Cho, C.K., Sah, D.W.Y., Stebbing, D., Crosley, E.J., Yaworski, E., Hafez, I.M., Dorkin, J.R., Qin, J., Lam, K., Rajeev, K.G., Wong, K.F., Jeffs, L.B., Nechev, L., Eisenhardt, M.L., Jayaraman, M., Kazem, M., Maier, M.A., Srinivasulu, M., Weinstein, M.J., Chen, Q., Alvarez, R., Barros, S.A., De, S., Klimuk, S.K., Borland, T., Kosovrasti, V., Cantley, W.L., Tam, Y.K., Manoharan, M., Ciufolini, M.A., Tracy, M.A., de Fougerolles, A., MacLachlan, I., Cullis, P.R., Madden, T.D., Hope, M.J., 2010. Rational design of cationic lipids for siRNA delivery. Nat. Biotechnol. 172. https://doi.org/10.1038/nbt.1602.

Vercauteren, D., Rejman, J., Martens, T.F., Demeester, J., De Smedt, S.C., Braeckmans, K., 2012. On the cellular processing of non-viral nanomedicines for nucleic acid delivery: mechanisms and methods. J. Control. Release 2, 566–581. https://doi.org/10.1016/j.jconrel. 2012.05.020.

Wang, X.L., Jensen, R., Lu, Z.R., 2007. A novel environment-sensitive biodegradable polydisulfide with protonatable pendants for nucleic acid delivery. J. Control. Release 120, 250–258. https://doi.org/10.1016/j.jconrel.2007.05.014.

Weecharangsan, W., Opanasopit, P., Ngawhirunpat, T., Apirakaramwong, A., Rojanarata, T., Ruktanonchai, U., Lee, R.J., 2008. Evaluation of chitosan salts as non-viral gene vectors in CHO-K1 cells. Int. J. Pharm. 348, 161–168. https://doi.org/10.1016/j.ijpharm.2007. 07.011.

Zhang, X.-X., Lamanna, C.M., Kohman, R.E., McIntosh, T.J., Han, X., Grinstaff, M.W., 2013. Lipid-mediated DNA and siRNA transfection efficiency depends on peptide headgroup. Soft. Matter. 17, 1–19. https://doi.org/10.1039/C3SM 27633C.

Zhou, C., Mao, Y., Sugimoto, Y., Zhang, Y., Kanthamneni, N., Yu, B., Brueggemeier, R.W., Lee, L.J., Lee, R.J., 2012. SPANosomes as delivery vehicles for small interfering RNA (siRNA). Mol. Pharm. 2, 201–210. https://doi.org/10.1021/mp200426h.